Supplemental Figure Legends

Figure S1. CC1736 expressed in the yeast *coq10* null mutant is detected in isolated mitochondria. Mitochondria were isolated from yeast *coq10* null mutants harboring the designated Coq10 homologues. Aliquots of mitochondria (50 μg of protein) were subjected to SDS-PAGE and Western blot analysis with antisera to the His-8 tag (*upper panel*). The slowest migrating His-tagged polypeptide is evident in the three right lanes is consistent with the predicted size of CC1736 precursor polypeptide harboring the unprocessed 35 amino terminal residues of Coq3 (17.8 kDa + 4 kDa). In the CC1736 and K115E lanes, the fastest migrating His-tagged polypeptide is consistent with predicted size of the mature CC1736 (17.8 kDa), while the middle band may represent an intermediate degree of processing. Antibodies to Atp2p were used as a loading control (*lower panel*).

Figure S2. Yeast *coq10* null mutants accumulate both unlabeled and $^{13}C_6$-labeled early Q_6-intermediates and show decreased content of Q_6 during early log phase growth. The experiment was performed as described in the legend to Fig. 8. The stacked bar graph depicts the $^{13}C_6$-labeled Q_6 and Q_6-intermediates (*green bars*), and unlabeled ^{12}C-Q_6 and ^{12}C-Q_6-intermediates (*blue bars*). The precursor-to-product ions are designated by *green text* for the $^{13}C_6$-labeled compounds, and *blue text* for the unlabeled ^{12}C-Q_6 and ^{12}C-Q_6-intermediates. Error bars depict the average ± standard deviation (n=4). The content of just the $^{13}C_6$-labeled Q_6 and $^{13}C_6$-labeled Q_6-intermediates was presented in Fig. 8. Statistical significance between pairs of samples for unlabeled ^{12}C-compounds (*blue bars*) was determined with the Student's t-test and lower-case letters above bars are indicative of statistical significance. In (*A*) and (*B*) the respective amounts of HAB or

HHB in the *coq10* null mutant at early-, mid-, or late-log phase growth were compared to the amounts present in the wild-type cells at the corresponding growth phase. ^{12}C-HAB and ^{12}C-HHB were significantly increased in the *coq10* null mutant extracts as compared to wild type (**a**, $p < 0.006$). For (*A*) and (*B*) the significance level α was adjusted to 0.0167 according to the Bonferroni correction. In (E) the content of unlabeled ^{12}C-Q_6 in the *coq10* null was compared to that present in wild-type cells at the corresponding growth phase (**a**, $p \leq 0.0006$). Additionally, unlabeled ^{12}C-Q_6 in mid- and late-log phase was compared to early-log phase for both wild type and the *coq10* null. Unlabeled Q_6 in wild type at mid-log phase was significantly different compared to early-log phase (**b**, $p \leq 0.0019$). For analyses of ^{12}C-Q_6 content in (*E*) the significance level α was adjusted to 0.0033 according to the Bonferroni correction. For comparisons of total Q_6 content (labeled $^{13}C_6$-Q_6 + unlabeled ^{12}C-Q_6) cultures containing $^{13}C_6$-ring precursors were compared to the ethanol control for the same strain and growth phase, (**c**, $p \leq 0.0045$). The significance level α was adjusted to 0.0083 according to the Bonferroni correction.

Figure S3. *De novo* synthesis of $^{13}C_6$-Q_6 and Q_6 content in yeast *coq10* null mutants in early log phase cultures is rescued upon transformation with *COQ10*, *CC1736* or *COQ8*. The designated yeast strains were cultured with one of aromatic ring precursors (^{13}C-4HB or ^{13}C-pABA), lipid extracts were prepared, and the amounts of endogenous Q_6 and Q_6-intermediates were detected as described in the legend to Fig. 9. The stacked bar graph depicts the $^{13}C_6$-labeled Q_6 and Q_6-intermediates (*green bars*), and unlabeled ^{12}C-Q_6 and ^{12}C-Q_6-intermediates (*blue bars*). The precursor-to-product ions are depicted in *green text* for the $^{13}C_6$-labeled compounds, and in *blue text* for the unlabeled ^{12}C-Q_6 and ^{12}C-Q_6-

intermediates. Error bars depict the average ± standard deviation (n=4). The content of just the $^{13}C_6$-labeled Q_6 and $^{13}C_6$-labeled Q_6-intermediates was presented previously in Fig. 9. Statistical significance between pairs of samples for the ^{12}C-unlabeled compounds (blue bars) was determined with the Student's t-test and lower-case letters above bars are indicative of statistical significance. In (*A*) the relative content of ^{12}C-unlabeled HAB in each of the *coq10* null transformants was compared to wild type (**a**, $p < 0.0001$). The relative content of ^{12}C-unlabeled HHB in (*B*) was similarly compared (**a**, $p \leq 0.0001$). The relative content of ^{12}C-unlabeled HAB or HHB between the *coq10* null with empty vector and the other *coq10* null transformants was also compared (**b**, $p \leq 0.0017$; note that *coq10Δ:CC1736* strain contained significantly higher content of HAB, while the transformants harboring either *COQ10* or *COQ8* contained lower amounts of HAB relative to the *coq10Δ* with empty vector. The significance level α was adjusted to 0.005 according to the Bonferroni correction for both (*A*) and (*B*). In (*E*) the content of unlabeled ^{12}C-Q_6 in each of the *coq10* null transformants was compared to wild type (**a**, $p \leq 0.0009$; note that the *coq10Δ:COQ8* strains contained significantly higher Q_6 content than wild type, while the other strains identified with a contained lower Q_6 content than wild type). The relative content of unlabeled ^{12}C-Q_6 between the *coq10* null transformed with empty vector and the three other *coq10* null transformants was also compared (**b**, $p < 0.0001$). For all analyses in (*E*) the significance level α was adjusted to 0.005 according to the Bonferroni correction.

Figure S4. *De novo* synthesis of $^{13}C_6$-Q_6 and Q_6 content in rescued yeast *coq10* null mutants in late log phase cultures is similar to that of wild-type yeast. The designated

yeast strains were cultured with one of the aromatic ring precursors (^{13}C-4HB or ^{13}C-pABA), as described in the Materials and Methods for detection of Q in concentrated cultures. Lipid extracts were prepared, and the amounts of endogenous Q_6 and Q_6-intermediates were detected as described in Fig. 8. The stacked bar graph depicts the $^{13}C_6$-labeled Q_6 (*green bars*), and unlabeled ^{12}C-Q_6 (*blue bars*). Precursor-to-product ions are depicted in *green text* for the$^{13}C_6$-Q_6, and in *blue text* for the unlabeled ^{12}C-Q_6. Error bars depict the average ± standard deviation. The differences in content of ^{12}C-Q_6 in the various strains were not significant. The content of $^{13}C_6$-Q_6 between the designated *coq10* null strain and wild type were significantly different (**a**, $p \leq 0.0013$). The content of $^{13}C_6$-Q_6 between the *coq10* null with empty vector and the other coq10 null transformants were significantly different (**b**, $p \leq 0.0025$). For all analyses the significance level α was adjusted to 0.005 according to the Bonferroni correction.

Figure S5. The mass of CC1736 and CC1736-K115E were determined with mass spectrometry. Spectra are shown for the purified CC1736 wild-type CC1736 polypeptide (WT) and the CC1736-K115E mutant polypeptide. The molecular mass of the isolated CC1736 and K115E polypeptides were determined by matrix-assisted laser desorption ionization (MALDI)-MS (DE-STR time-of-fight instrument, Applied Biosystems) to be 17841.0 ± 1.1 Da and 17842.4 ± 0.8, respectively. Both are in agreement with the theoretical masses of 17842.4 Da and 17843.4 predicted from the respective amino acid sequences. For the tryptic digests, the WT shows the tryptic peptides corresponding to residues 106-115 and 116-129 from the Lys at position 115. The K115E mutant,

however, shows instead a tryptic peptide for residues 106-129 (and separate peptides for 106-115 and 116-129 are absent).

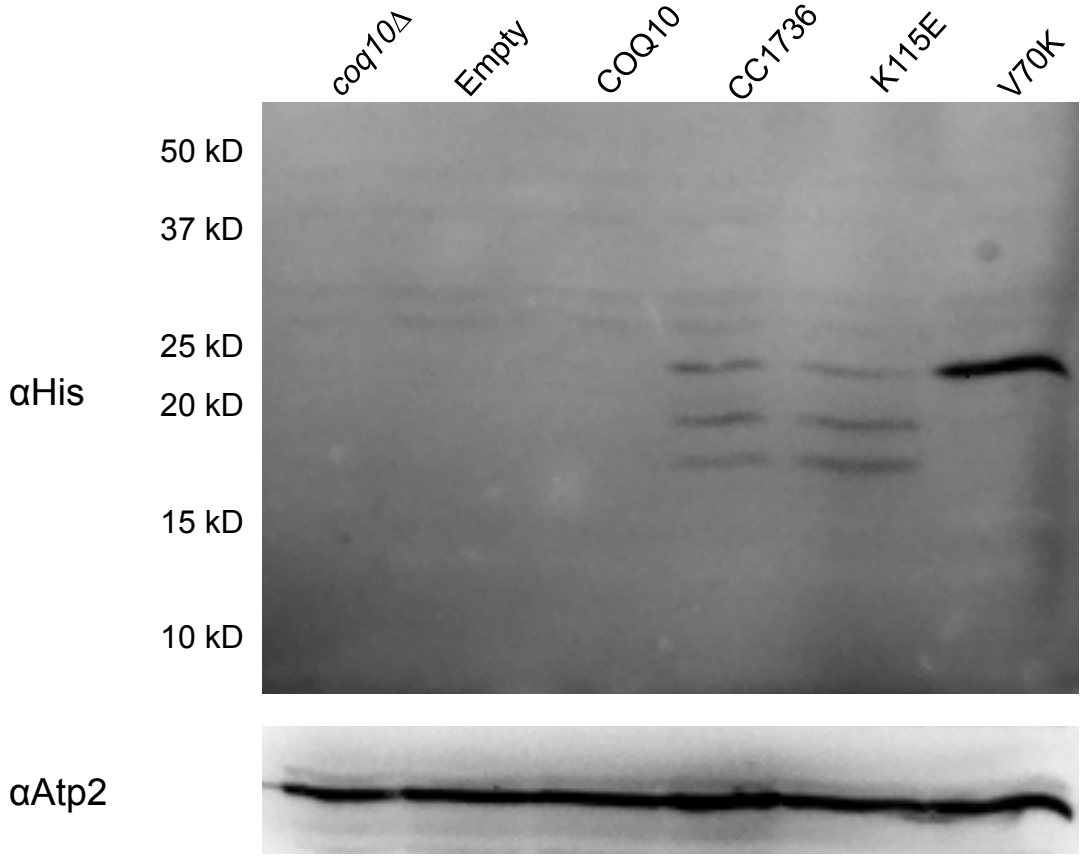
coq10Δ
Empty
COQ10
CC1736
K115E
V70K
50 kD
37 kD
25 kD
20 kD
15 kD
10 kD
αHis
αAtp2

Fig. S1

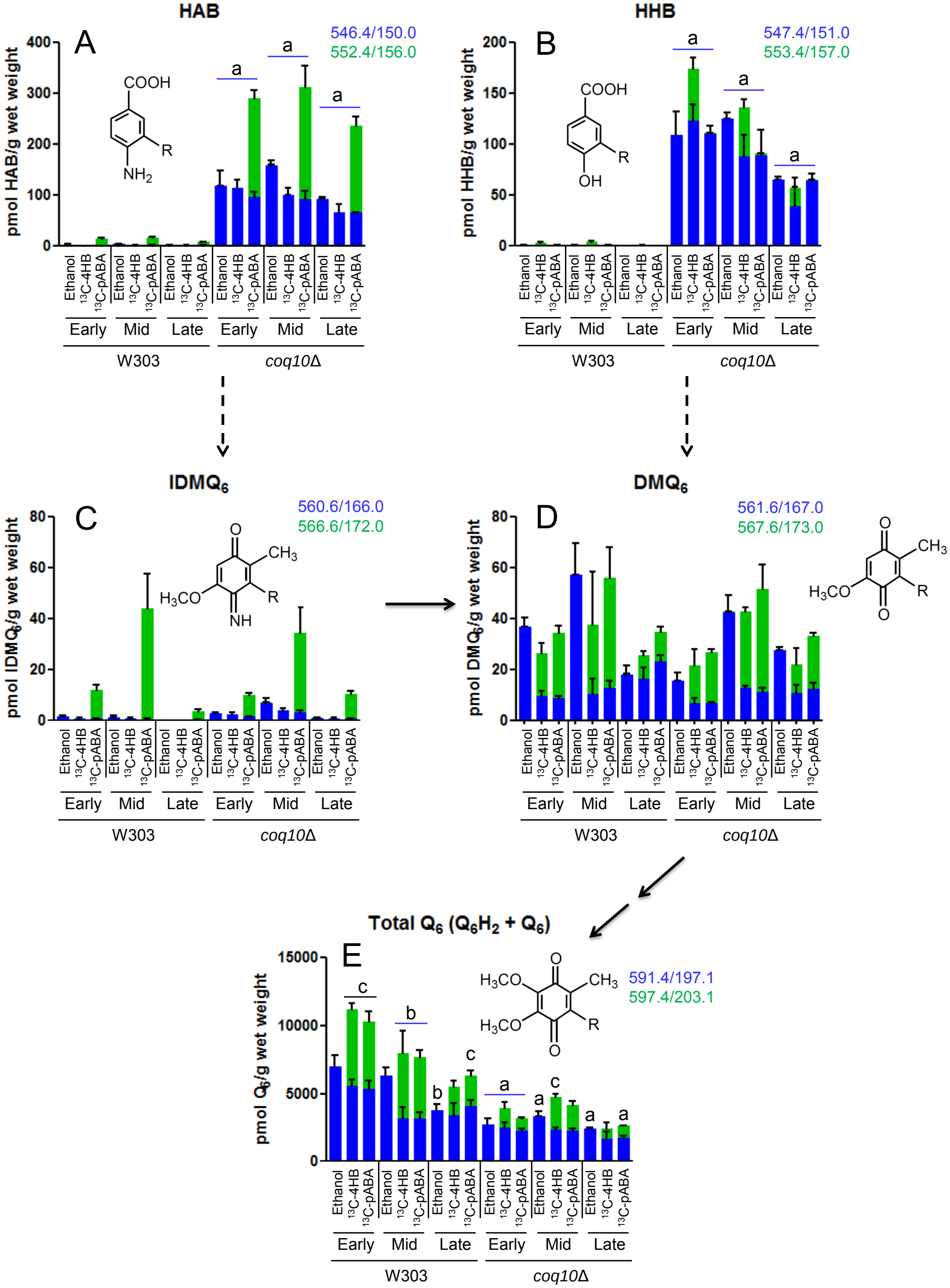
HAB
A
546.4/150.0
552.4/156.0
pmol HAB/g wet weight
COOH
R
NH2
a
a
a
HHB
B
547.4/151.0
553.4/157.0
pmol HHB/g wet weight
COOH
R
OH
a
a
a
Ethanol
13C-4HB
13C-pABA
Early
Mid
Late
W303
coq10Δ
IDMQ6
C
560.6/166.0
566.6/172.0
pmol IDMQ6/g wet weight
O
CH3
H3CO
R
NH
DMQ6
D
561.6/167.0
567.6/173.0
pmol DMQ6/g wet weight
Total Q6 (Q6H2 + Q6)
E
pmol Q6/g wet weight
591.4/197.1
597.4/203.1
H3CO
CH3
H3CO
R
c
b
b
c
a
a
c
a
a

Fig. S2

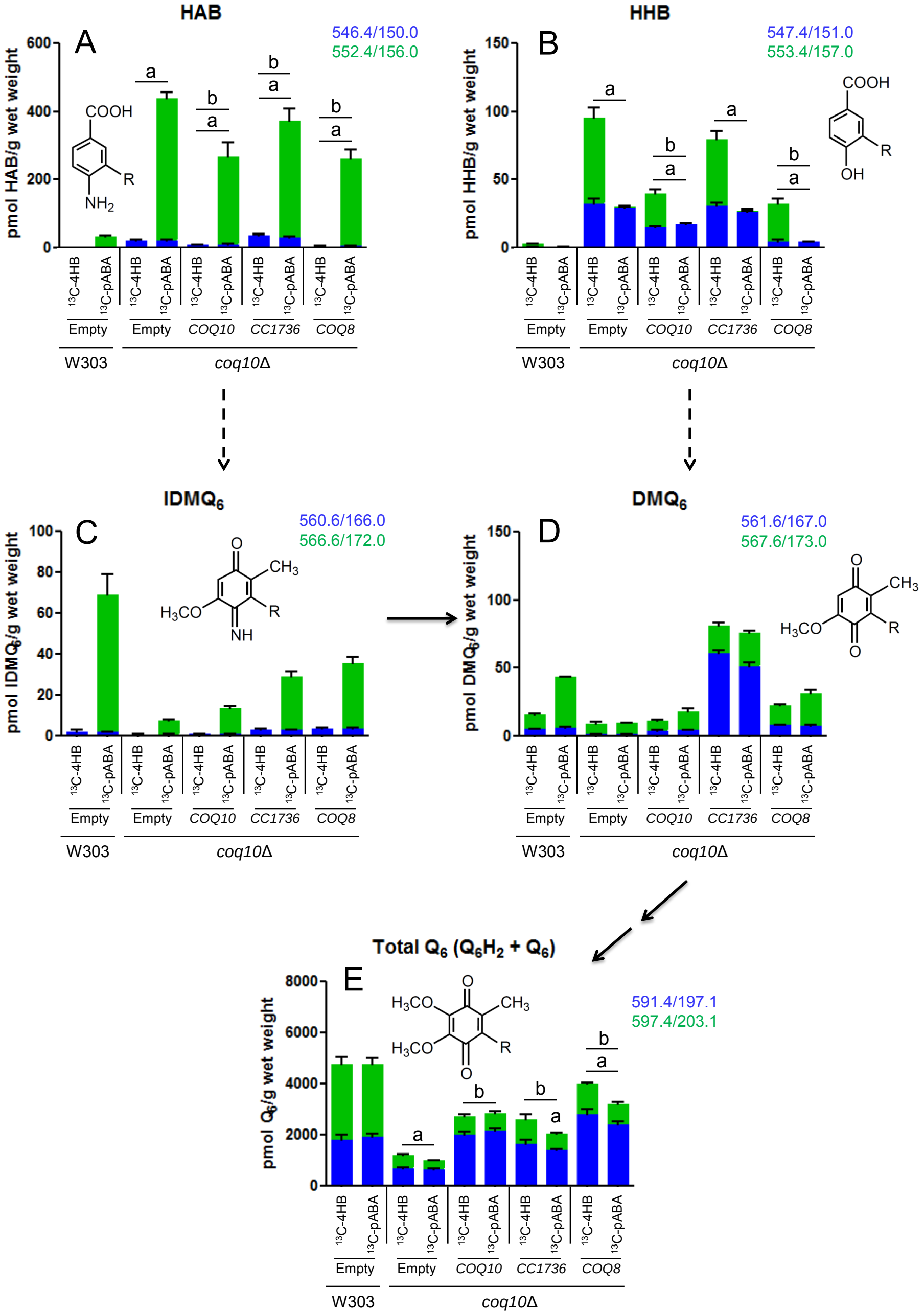
HAB
A
546.4/150.0
552.4/156.0
pmol HAB/g wet weight
COOH
R
NH2
HHB
B
547.4/151.0
553.4/157.0
pmol HHB/g wet weight
COOH
R
OH
IDMQ6
C
560.6/166.0
566.6/172.0
pmol IDMQ6/g wet weight
O
CH3
H3CO
R
NH
DMQ6
D
561.6/167.0
567.6/173.0
pmol DMQ6/g wet weight
Total Q6 (Q6H2 + Q6)
E
591.4/197.1
597.4/203.1
pmol Q6/g wet weight
13C-4HB
13C-pABA
Empty
COQ10
CC1736
COQ8
W303
coq10Δ

Fig. S3

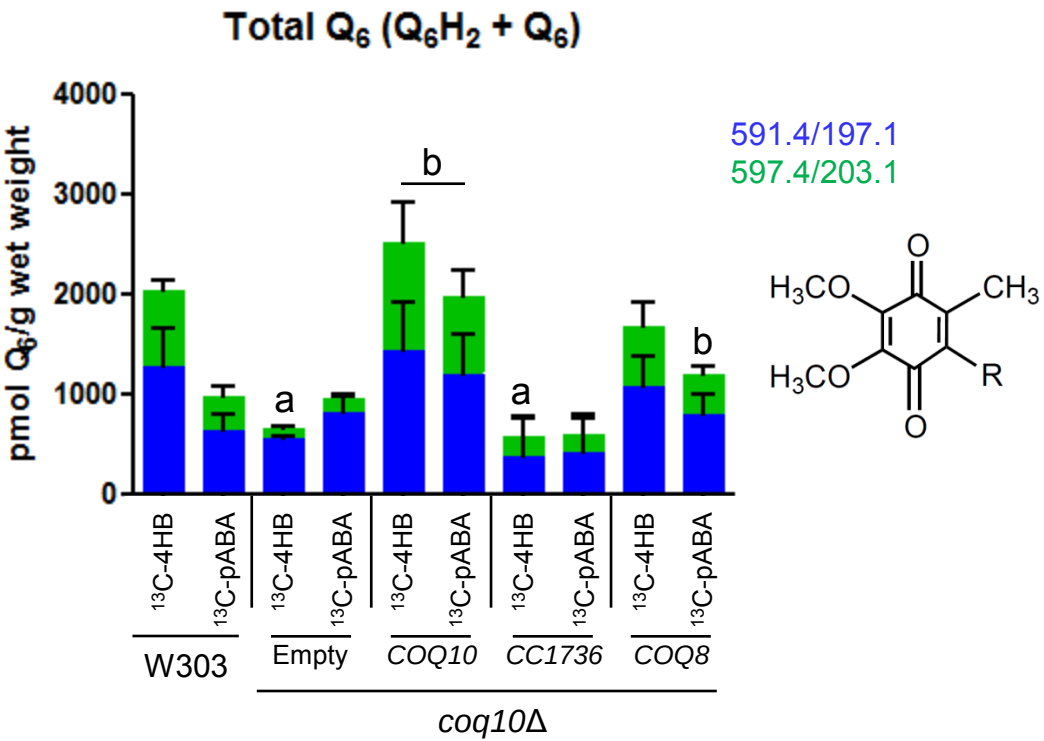
Total Q_6 (Q_6H_2 + Q_6)
pmol Q_6/g wet weight
4000
3000
2000
1000
0
a
b
a
b
591.4/197.1
597.4/203.1
H_3CO
CH_3
H_3CO
R
O
O
^{13}C-4HB
^{13}C-pABA
W303
Empty
COQ10
CC1736
COQ8
coq10Δ

Fig. S4

MALDI-MS

intact protein and trypsin digest

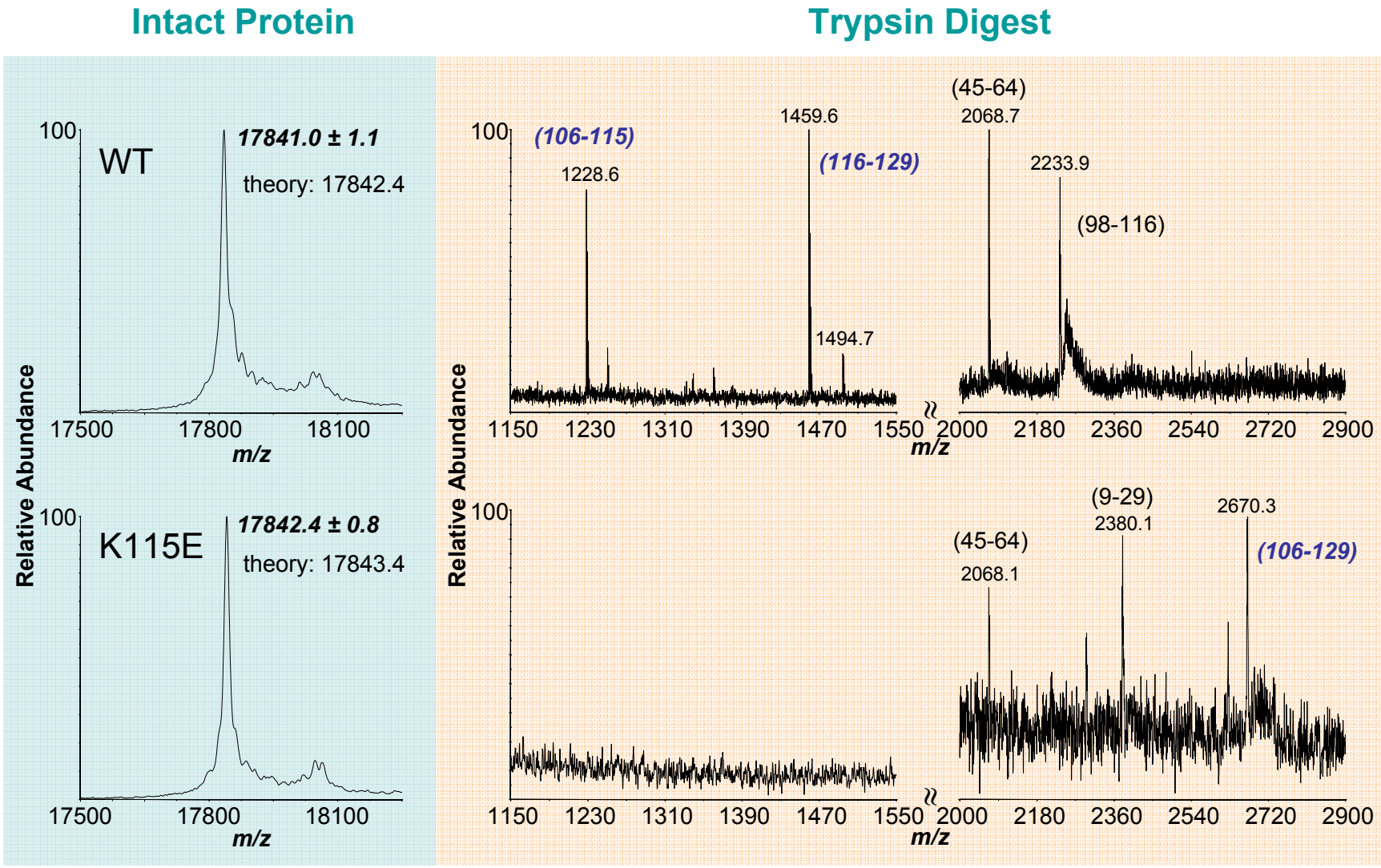

Fig. S5